HAL
open science

Simulation of dispersed flow film boiling in LOCA conditions considering different fuel rod blockage ratios

Juan Esteban Luna Valencia, Tony Glantz, Arthur V S Oliveira, Alexandre Labergue, Michel Gradeck

To cite this version:

Juan Esteban Luna Valencia, Tony Glantz, Arthur V S Oliveira, Alexandre Labergue, Michel Gradeck. Simulation of dispersed flow film boiling in LOCA conditions considering different fuel rod blockage ratios. 19th International Topical Meeting on Nuclear Reactor Thermal Hydraulics (NURETH-19), ANS, Mar 2022, Virtual Meeting, Belgium. hal-03727179

HAL Id: hal-03727179

https://hal.univ-lorraine.fr/hal-03727179v1

Submitted on 19 Jul 2022

HAL is a multi-disciplinary open access archive for the deposit and dissemination of scientific research documents, whether they are published or not. The documents may come from teaching and research institutions in France or abroad, or from public or private research centers.

L'archive ouverte pluridisciplinaire **HAL**, est destinée au dépôt et à la diffusion de documents scientifiques de niveau recherche, publiés ou non, émanant des établissements d'enseignement et de recherche français ou étrangers, des laboratoires publics ou privés.

Copyright

The 19th International Topical Meeting on Nuclear Reactor Thermal Hydraulics (NURETH-19) Log nr.: 19001
Brussels, Belgium, March 6 - 11, 2022

SIMULATION OF DISPERSED FLOW FILM BOILING IN LOCA CONDITIONS CONSIDERING DIFFERENT FUEL ROD BLOCKAGE RATIOS

J.E. Luna Valencia and T. Glantz
IRSN
B.P. 3, 13115 Saint Paul-Lez-Durance, France
juan-esteban.luna@irsn.fr; tony.glantz@.irsn.fr

A.V.S. Oliveira, A. Labergue, M. Gradeck
Université de Lorraine
CNRS, LEMTA, F-54000 Nancy, France
arthur.oliveira@univ-lorraine.fr; alexandre.labergue@univ-lorraine.fr; michel.gradeck@univ-lorraine.fr

ABSTRACT

During a loss of coolant accident (LOCA), in a nuclear-pressurized water reactor, fuel assemblies can be damaged and water is injected to cool down the core. In this hypothetical situation, a dispersed flow of steam and droplets occurs downstream of the quenching front. This two-phase flow propagates through the assemblies which can be deformed due to the swelling of the fuel rods' cladding causing blocked sub-channels. This complex flow plays an important role in the initial cooling of fuel rods that are not yet immersed into water. However, blocked sub-channels cooling is degraded because of the preferential steam flow towards less blocked regions. In previous work, we presented a mechanistic model implemented in the NECTAR code, which calculates heat and mass transfer phenomena as well as droplets dynamics in a polydispersed flow film boiling. NECTAR was validated with experimental measurements using three different geometries representing the cladding ballooning at a sub-channel scale. The French Institut de Radioprotection et de Sûreté Nucléaire (IRSN) has recently performed measurements of flow redistribution in a 7×7 fuel rods bundle with 4×4 ballooned rods under different geometric conditions (blockage ratio, length, and coplanarity), as well as different flow rates, showing that the blockage ratio is the predominant factor in the amount of deviated flow. In this article, we analyze the influence of the steam deviation on the heat transfer in a blocked sub-channel, with different blockage ratios (61% and 90%) and lengths (100 mm and 300 mm) for representative LOCA conditions. The internal heat dissipation is evaluated and the contributions of the different involved mechanisms are analyzed.

KEYWORDS
LOCA, Nuclear reactor, Clad ballooning, Thermal-hydraulics, Mechanistic model, NECTAR

1. INTRODUCTION

After a LOCA, the safety systems inject water into the nuclear core plenum with the objective to prevent nuclear rods from reaching safety limit temperatures and thus mitigate the accident consequences. During this phase called "re-flooding", the injected water comes into contact with the nuclear rods at high temperatures producing a complex flow of steam and dispersed droplets downstream the quenching front. At this phase, this dispersed flow serves as a coolant for the nuclear rod section downstream the quenching front. At the same time, some nuclear rods can undergo large deformations, leading to a decrease in the fluid passage area of some sub-channels. As a result, the effectiveness of security systems can be compromised. Furthermore, these blocked sub-channels cause the steam to deviate to the less blocked sub-channels [1,2]. Consequently,

the cooling of blocked sub-channels can be compromised because forced convection with steam is supposed to be the dominant phenomenon in the cooling of the assembly [3]. On the other hand, Ruyer et al. [4] found that droplets show an inertial behavior and do not deviate with the steam. Subsequently, the droplets could improve the cooling of these blocked sub-channels. Thus, understanding this phenomenon is a major issue for nuclear safety design. However, the physical characterization of this flow involves complex and intricate phenomena such as droplets fragmentation and coalescence, turbulence, droplets interactions or impacts onto the wall, and also thermodynamic non-equilibrium between phases. Figure 1 represents the main thermal-hydraulic phenomena downstream of the quenching front. Additionally, Table 1 shows the range of some thermal-hydraulic parameters considered in this two-phase flow [5–7]. Furthermore, previous studies indicate that the liquid droplet size distribution in this two-phase flow can be adequately represented by a log-normal distribution [5–8].

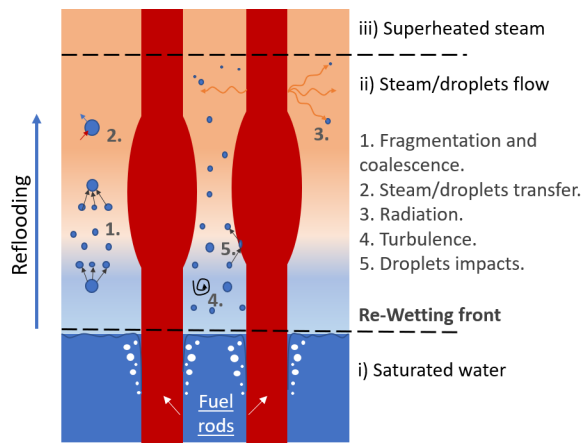

Figure 1. Heat and mass transfer phenomena in LOCA. [3].

Table I. Typical values during a LOCA.

Parameter	Typical value during LOCA
Droplets diameter (d_g)	50 μm - 1300 μm
Droplets velocity (u_g)	4 m/s - 16 m/s
Droplets volume fraction (α)	10^{-4} - 10^{-2}
Steam Temperature (T_s)	$< 800\ °C$
Wall Temperature (T_w)	300 $°C$ - 1200 $°C$

For this reason, and intending to support safety analysis of pressurized water reactors, the IRSN has developed a code, name DRACCAR *, capable of describing the fuel assemblies' behavior during a LOCA. To do so, DRACCAR calculates the thermal-hydraulics in all the reactor circuits and the thermo-mechanical be-

*DRACCAR: **D**éformation et **R**enoyage d'un **A**ssemblage de **C**rayons **C**ombustibles pendant un **A**ccident de **R**efroidissement.

havior of fuel assemblies [9]. Moreover, the IRSN has launched several experimental campaigns that serve to validate DRACCAR code. In the thermal-hydraulics axis, the main experiment (named COAL[†] [10, 11]) consists of a 7 x 7 bundle of electrically heated rods at a full-length scale, with a blocked region by the presence of clad ballooning in the bundle. In this way, COAL experiments give useful information about the thermal-hydraulics phenomena during the re-flooding phase in a bundle scale. However, information on the heat transfer between the rods and the two-phase flow at the sub-channel scale is not well characterized. Consequently, another experiment, named COLIBRI [‡], was developed to accurately characterize the thermal-hydraulic phenomena downstream of the re-wetting front at a sub-channel scale. The COLIBRI experimental bench consists of a test section of a single heated tube and a supply system of droplets and super-heated steam [5].

Additionally to COLIBRI bench, a mechanistic model in a numerical code was also developed, named NECTAR[§], in order to calculate the heat and mass transfers involved between the polydisperse flow and the high-temperature nuclear rods at the scale of a subchannel. Additionally, NECTAR calculates as well the droplets dynamics. One of the characteristics of this 1D code is that it considers the droplets' distribution, the droplets' dynamics in the steam core, and the droplets' fragmentation. NECTAR has been first validated by experimental measurements carried out on the COLIBRI experimental bench [5], for three different geometries representing the cladding swelling at the sub-channel scale and different thermal-hydraulic conditions [3].

In addition, the IRSN carried out measurements of the redistribution flow rate in a 7 × 7 assembly with 16 ballooned rods for different geometric conditions (blockage ratio, blockage length, and coplanarity of the deformation) as well as for different flow rates and without heat transfer between the flow and the wall. The results showed that the blockage ratio plays a major role in the flow redistribution and as a result, the amount of deviated flow is proportional to the blockage rate. This blockage ratio (τ_b), defined in Eq. 1, is a parameter used to characterize the reduction in the cross-section due to the deformation of the cladding in a LOCA; where S_b and S_0 are, the cross-sectional area of a blocked and an intact sub-channel respectively.

$$\tau_b = 1 - \frac{S_b}{S_0}, \quad \tau_{b(90\%)} = 0.9, \quad \tau_{b(61\%)} = 0.61 \tag{1}$$

The experimental results obtained with COLIBRI have shown an improvement in heat transfer in the case of a blocked sub-channel, owing to the steam acceleration (i.e. not deviated) in the blocked sub-channels. As the steam mass flow rate entering the test section was kept equal in all cases, the steam velocity, therefore, increased due to a Venturi effect. For this reason, the COLIBRI bench has been modified to account for the effect of flow redistribution within a more realistic assembly. With the aim of estimate the thermal-hydraulic behavior of these new experiments, we present a simulation of the dispersed flow film boiling by considering this steam flow deviation using NECTAR for two blockage ratios ($\tau_b = 61\%$ and 90%) and lengths (100 mm and 300 mm) to be used in COLIBRI bench.

2. NECTAR CODE

The code is based on the heat balance between the nuclear rod (hot wall to be cooled) and the internal flow of superheated steam and dispersed droplets. NECTAR uses an 1D axial model of steam and droplets in thermal

[†]COAL: **CO**olability of a fuel **A**ssembly during **L**OCA
[‡]COLIBRI: **CO**oLIng of **B**lockage **R**egion **I**nside a PWR Reactor.
[§]NECTAR: **N**ew **E**xperimental **C**ode for **T**hermal-hydraulic **A**nalysis in a **R**epresentative geometry.

and dynamic non-equilibrium. The droplets are considered to be spherical and at saturation. Figure. 2 shows the different transfers: forced wall/steam convection ($\Phi_{c,ws}$), wall/steam radiation ($\Phi_{r,ws}$), steam/droplets convection ($\Phi_{c,sd}$), steam/droplets radiation ($\Phi_{r,sd}$), wall/droplets radiation ($\Phi_{r,wd}$), wall/droplets impacts ($\Phi_{i,wd}$) and evaporation of droplets (m_{ev}).

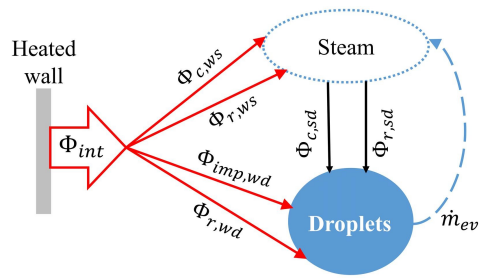

Figure 2. Heat and mass transfer paths considered in NECTAR [3].

The dissipated heat flux at the wall due to the internal flow (Φ_{int}) is therefore the sum of four different contributions:

$$\Phi_{int} = \Phi_{c,ws} + \Phi_{r,ws} + \Phi_{imp,wd} + \Phi_{r.wd} \tag{2}$$

For the calculation of the different heat transfer mechanisms NECTAR uses the following correlations:

- Gnielinski correlation [12], for the forced wall/steam convection ($\Phi_{c,ws}$) :

$$Nu_s = \frac{f/8\,(Re_s - 1000)\,Pr}{1 + 12.7(f/8)^{1/2}\,(Pr^{2/3} - 1)} \tag{3}$$

- For the steam/droplets convection ($\Phi_{c,sd}$), the Ranz and Marshall correlation [13] with the modification of Yuen and Chen [14]:

$$Nu_{sd}\,(1 + (h_s - h_d)\,/h_{fg}) = 2 + 0.6Re_M^{1/2}Pr_f^{1/3} \tag{4}$$

- Impacts of droplets onto the wall ($\Phi_{imp,wd}$). The code uses the data (for the estimation of h_i) and the model from Gradeck et al. [15] for the calculation of the energy taken by a single drop:

$$E_d = \int_0^{t_s} \left(h_i\,(T_w - T_s) + \varepsilon_w \sigma_{SB}\left(T_w^4 - T_d^4\right)\right) \frac{\pi d\,(t)^2}{4} dt \tag{5}$$

  Where h_i, ε_w, $d(t)$ and σ_{SB} represent the transfer coefficient by the impact of a drop, the emissivity of the wall, the droplet diameter, and the Stefan Boltzmann's constant respectively. The Biance et al. model [16] was used to calculate the droplet diameter during impact ($d(t)$). Additionally, the total heat flux extracted by droplets impacts $q_{imp,wd}$ can be estimated as:

$$q_{imp,wd} = \frac{6\dot{m}}{\pi \rho_d d^3} E_d \tag{6}$$

Where $\dot{m}$ is the mass flux density of droplets impinging the wall. Moreover, NECTAR code estimates this mass flux with Hewitt et Govan [17] correlation for droplet deposition rate, with the correlation used by Guo et Mishima [18] to estimate the concentration of the droplets in the steam core:

$$\dot{m} = \frac{0.18}{\sqrt{\rho_s D_h/\sigma_t}}\alpha\rho_d \quad if \;\; \alpha\rho_d/\rho_s < 3, \quad \frac{0.083(\alpha\rho_d/\rho_s)^{-0.65}}{\sqrt{\rho_s D_h/\sigma_t}}\alpha\rho_d \quad if \;\; \alpha\rho_d/\rho_s > 3 \tag{7}$$

- For the radiation heat transfer calculation between the steam, the droplets and the wall, the code uses the thermal resistance model of Sun et al. [19]. The radiation heat flux between each phase can be expressed as:

$$q_{r,ij} = F_{r,ij}\sigma_B(T_i^4 - T_j^4) \tag{8}$$

Where $F_{r,ij}$ is the form factor, defined as

$$F_{r,ij} = 1/\left(R_i + R_j + R_i R_j/R_k\right) \tag{9}$$

Where the indices i, j and k represent each phase (steam, droplets or the wall). Finally, the thermal resistance R of each phase is expressed as

$$R_s = (1-\varepsilon_s)\,/\left[\varepsilon_s\left(1-\varepsilon_s\varepsilon_d\right)\right] \tag{10}$$

$$R_d = (1-\varepsilon_d)/\left[\varepsilon_d(1-\varepsilon_s\varepsilon_d\right] \tag{11}$$

$$R_w = 1/(1-\varepsilon_s\varepsilon_d) + (1-\varepsilon_w)/\varepsilon_w \tag{12}$$

Table 1 summarizes the conservation equations used in NECTAR. Furthermore, the volumetric evolution of the dispersed phase (i.e. the droplets) is determined according to the moment density equations [5], [11] described along the vertical z-axis. The model does not consider the coalescence of the droplets; however, fragmentation of the droplets is possible. For this, the Chou and Faeth model [20] is used to calculate the new distribution after fragmentation. Moreover, the wall is considered to be thermally "thin" (Bi $\ll$ 1) and the simulations are only valid in the Leidenfrost regime.

Table II. Conservation equations of the NECTAR code [3].

	Equations
Mass conservation (steam)	$\frac{\mathrm{d}m_s}{\mathrm{d}t} = \dot{m}_{ev}$
Momentum balance (droplet)	$\rho_d u_d \frac{\mathrm{d}u_d}{\mathrm{d}z} = \frac{3}{4d}\frac{v.C_D}{1+B}\rho_s\left(u_d - u_s\right)\left\|u_d - u_s\right\| + \left(\rho_s - \rho_d\right)g$ $C_D = \frac{24}{Re(1+B)}, B = \frac{Cp_s(T_s - T_{sat})}{h_{fg} + (Q_L/\dot{m}_d)}, v = \frac{1}{1-6.55\alpha_d}$
Energy balance	$Cp_s\left\{T_s\left(z+dz\right)\left[\dot{m}_s(z) + \frac{\mathrm{d}\dot{m}_s(z)}{\mathrm{d}t}\right] - \dot{m}_s(z)T_s(z)\right\} = \Phi_{ev}$ $\Phi_{ev} = \Phi_{imp,wd} + \Phi_{r,wd} + \Phi_{sd} + \Phi_{r,sw}$

3. SIMULATION DOMAIN AND BOUNDARY CONDITIONS

Figure. 3 shows the simulation domain and the boundary conditions of the NECTAR simulation. The code uses the same geometry of the COLIBRI experimental bench, described by Peña Carrillo et al. [5], which represents a blocked fluid sub-channel as a circular section venturi. As explained by Peña Carrillo et al. [5], this choice of geometry allows to accurately assess the heat transfers paths in this mist flow at the sub-channel scale, providing valuable information for DRACCAR's code validation.

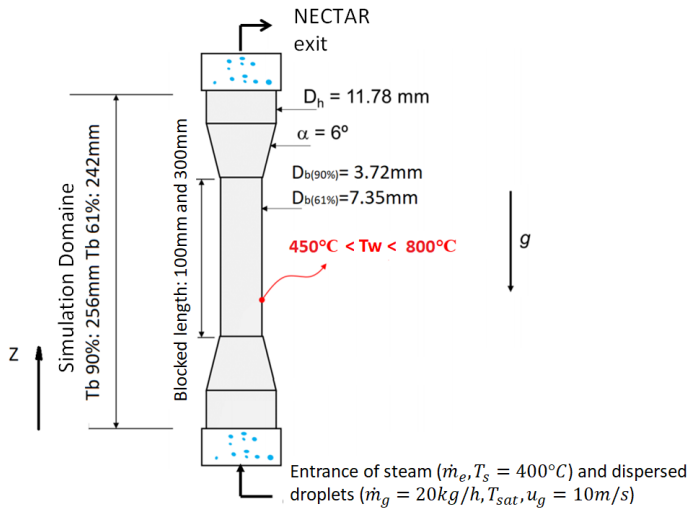

Figure 3. Simulation Domain of NECTAR simulation.

Oliveira et al. [1, 2] found that the blockage ratio plays a major role on the flow redistribution in a bundle with blocked sub-channels. Additionally, they found that the amount of deviated flow is proportional to the blockage ratio. Therefore, for the present work, the amount of deviated steam is taken as proportional to the blockage ratio (according to Eq. 1).

$$\dot{m}_e = (1 - \tau_b)\dot{m}_0 \tag{13}$$

According to the results of Oliveira et al. [1,2] and Ruyer et al. [4], the steam deviation is carried out up to the transition zone between the intact and blocked section, however, in the COLIBRI experimental bench, the deviation is carried out in a single point immediately before the transition zone (out of NECTAR simulation domain). Consequently, the steam mass flow entering the COLIBRI test section has been already deviated (reduced). For this reason, before the thermal calculation, the NECTAR code determines the steam mass flow rate according to Eq. 13.

Finally, in order to simulate the new experimental conditions of the COLIBRI experimental bench, the following input conditions have been set : (1) wall temperatures between 450°C and 800°C, (2) initial mass flow rate of steam ($\dot{m}_0$) of 4 kg/h, at 1 bar (absolute pressure) and at 400°C of temperature and (3) droplets mass flow rate of 20 kg/h, which corresponds to a volume fraction of 5.10^{-3}. The initial droplets velocity is 10 m/s. The droplets distribution is log-normal, as shown in Fig. 4. The average diameter d_{10} is 250 μm, for a maximum diameter of 700 μm and a minimum diameter of 5 μm. In this study, we chose two different

blockage ratios with two different blockage lengths, named 61%/100mm, 61%/300mm, 90%/100mm, and 90%/300mm; with this notation, the first value (before the slash) of the notation corresponds to the simulated blockage ratio and the second one (after the slash) correspond to the simulated blocking length. Finally, the droplets' distribution used is typical in LOCA case. Nevertheless, this parameter depends on other factors, such as the mass flow of steam. Therefore, it is not possible to exactly fix a droplet distribution for the COLIBRI experimental bench. However, although there is an increase in the heat flux removed from the wall with an increase in the droplets' diameter, this is not significant (as is the increase in the mass flow of droplets or steam) [21].

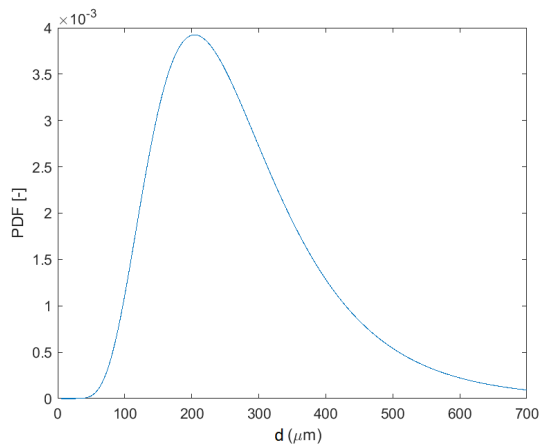

Figure 4. Log-normal droplets distribution (μ=0.45, σ= ln(d_{10}), d_{10}=250μm).

4. RESULTS

We present herein the results of internal heat flux per unit of blocked length for the chosen blockage ratios ($\tau_b = 61\%$ and $\tau_b = 90\%$) and lengths (100 mm and 300 mm) with and without flux deviation (bypass). As expected, there is a decrease in heat transfer when there is a steam deviation for both blockage lengths simulated (Fig. 5 and Fig. 6). On the other hand, there is a small difference in the heat flux released by the wall between the two blockage ratios when the steam deviation is simulated. For the cases with a more severe blockage length (300 mm), this difference is even smaller (Fig. 6). This is due to an slight increase in heat transfer by droplets impacts ($\Phi_{imp,wd}$), in the most blockage case.

Table III summarizes the heat flux per unitary blockage length for each mechanism of heat transfer. In general, the results show a slight increase in the internal heat flux (Φ_{int}) per blocked length for the cases of 300 mm of blockage length. This is due to an improvement in convective heat transfer between the steam and the wall ($\Phi_{c,ws}$). Also, a decrease in droplets impacts heat transfer (c) is evidenced while increasing blockage length. On the other hand, when comparing the results with and without steam deviation, a reduction in heat flow is highlighted. However, this reduction is cushioned by the increase in heat transfer due to droplets impacts ($\Phi_{imp,wd}$) and by the decrease in the steam temperature that favors wall/steam convection ($\Phi_{c,ws}$) (Fig. 7). This means that the decrease in heat transfer between the steam and the wall is damped because even though the heat transfer coefficient was reduced (by reducing the mass flow), the temperature difference increased. Consequently, the decrease in heat is not proportional to the decrease in the steam mass flow. Furthermore, this reduction in steam temperature is due to convective heat transfer between the steam and the droplets ($\Phi_{c,sd}$).

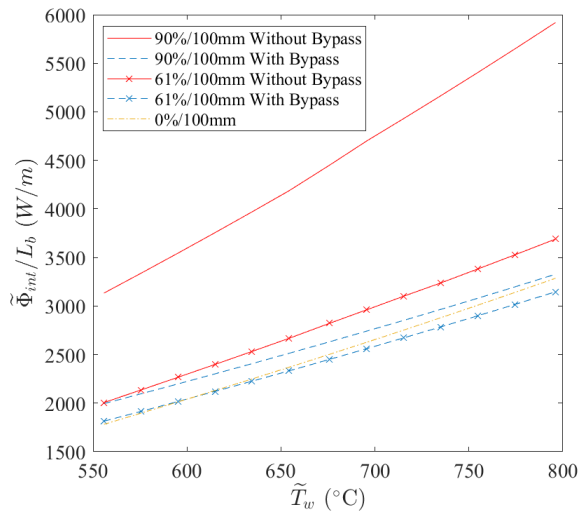

Figure 5. Internal heat flow as a function of the average wall temperature for the cases with a 100mm blockage length.

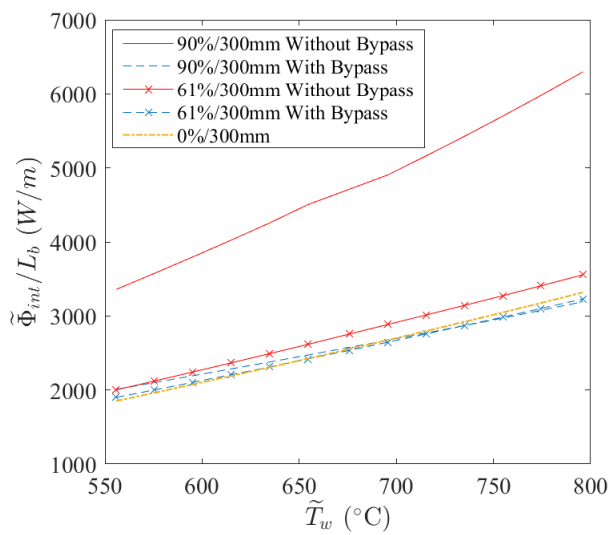

Figure 6. Internal heat flow as a function of the average wall temperature for the cases with a 300mm blockage length.

A discontinuity in the steam temperature is evidenced in Fig. 7 for the cases without steam deviation. This is due to the droplets' fragmentation in the blocked zone. In this way, the importance of droplets is seen in the wall cooling. On the other hand, the influence of the droplets can also be evidenced on the heat transfer with the wall, when even for the cases without blockage ($\tau_b = 0\%$), the droplets' impact heat transfer mechanism ($\Phi_{imp,wd}$) is the most important for both blockage length ratio simulated. Furthermore, this same behavior is reflected for blocked sub-channels when there is steam deviation, where ($\Phi_{imp,wd}$) represents more than half of the total heat flow contribution. These results will be compared with experimental results that will be obtained soon in the new campaign with the experimental bench COLIBRI.

Table III. Internal heat flux per blockage length for the studied cases (W/o BYP: without bypass and W/ BYP: with bypass).

Heat Transfer Mech.	Internal heat flux per blockage length $[kW/m]$									
	τ_b = 0%		τ_b = 61%				τ_b = 90%			
	100mm	300mm	100mm		300mm		100mm		300mm	
	W/o BYP	W/o BYP	W/ BYP	W/o BYP	W/ BYP	W/o BYP	W/ BYP	W/o BYP	W/ BYP	W/o BYP
$\Phi_{imp,wd}$	1.25 *49%*	1.21 *46,5%*	1.4 *56,2%*	1,01 *34,8%*	1,35 *52,1%*	0,88 *31,3%*	1,63 *60.83%*	0,26 *5,6%*	1,32 *50,6%*	0,205 *4,3%*
$\Phi_{c,ws}$	1.02 *40%*	1.14 *43.4%*	0.85 *33.9%*	1.64 *56.6%*	1.02 *39.2%*	1.74 *61.6%*	0.84 *31.2%*	3.97 *87.4%*	1.09 *41.9%*	4.4 *94.5%*
$\Phi_{r,wd}$	0,19 *7.57%*	0,17 *6.71%*	0,2 *8.05%*	0,20 *7.04%*	0,18 *6.83%*	0,15 *5.46%*	0,19 *7.22%*	0,3 *6.55%*	0,17 *6.67%*	0,187 *3.9%*
$\Phi_{r,ws}$	0,09 *3.38%*	0,09 *3.42%*	0,05 *1.91%*	0,05 *1.54%*	0,05 *1.91%*	0,05 *1.59%*	0,02 *0.72%*	0,02 *0.37%*	0,02 *0.74%*	0,02 *0.35%*
Φ_{int}	2,56	2,61	2,5	2,89	2,60	2,83	2,68	4,53	2,6	4,81

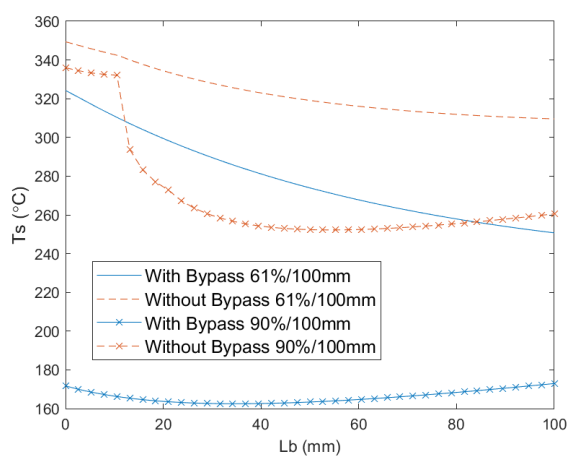

Figure 7. Steam temperature in the blocked zone for 61%/100mm and 90%/100mm (Tw=607°C).

5. CONCLUSIONS

The simulations carried out with NECTAR code allows the analysis of the influence of steam deviation on the heat transfer which take place in a representative tube of a PWR sub-channel cooled by a steam flow with dispersed droplets during a LOCA. This analysis yielded the following results:

- The steam-to-wall convection ($\Phi_{c,ws}$) was reduced with the reduction of the mass flow. However, the heat transfer between the droplets and the steam ($\Phi_{c,sd}$) caused the steam temperature to be lower

than in the non-deviation cases. Consequently, the reduction in heat exchange between the wall and the steam was not proportional to the steam mass flow reduction.

- Increasing the blockage length slightly improves heat transfer in the presence of steam deviation. However, in the simulations carried out the blockage length is not an influencing factor in the sub-channels cooling.
- The droplets have an important role in the sub-channel cooling for the droplets fraction volume studied. This is reflected in the importance of heat transfer by droplets impact onto the wall ($\Phi_{imp,wd}$) for the cases with steam deviation and the cases without blockage. Additionally, the droplets decrease the steam temperature, thus improving the heat transfer with the wall.

These numerical results obtained with NECTAR should be validated experimentally with the new COLIBRI experimental campaign. In addition, given the great influence of droplets on cooling, it is necessary to take into account for the possible effect of droplets' interactions on the different heat transfers.

ACKNOWLEDGMENTS

This work is carried out as part of a PhD thesis funded by the Institut de Radioprotection et de Sûreté Nucléaire (IRSN) in Cadarache, France.

NOMENCLATURE

Latin letters

Cp	Specific Heat at constant pressure [J/kgK]
d	Droplet diameter [m]
D_h	Hydraulic diameter [m]
E_d	Energy single droplet [J]
f	Friction coefficient
F_r	Radiation form factor
g	Gravity [m/s^2]
h	Enthalpy [J/Kg]
h_i	Heat transfer coefficient of a droplet impact [W/m^{2}K]
m	Mass [kg]
$\dot{m}$	Mass flux density [kg/m^{2}s]
$\dot{m}_e$	Inlet steam mass flow [kg/s]
$\dot{m}_0$	Initial steam mass flow [kg/s]
Pr	Prandtl number
q	Heat flux [W/m^2]
Re	Reynolds number
S_b	Blocked cross-section area
S_0	Intact cross-section area
T	Temperature [K]
t	Time [s]
u	Velocity [m/s]
We	Weber number
z	Axial axis

Greek letters

α	Volume fraction
μ	Log-normal mean
Φ	Rate of heat flow
ρ	Density [kg/m^3]
σ	Log-normal variance
σ_t	Surface tension [N/m]
σ_B	Stephan-Boltzmann constant
τ_b	Blockage ratio
ε	Emissivity
ν	Kinematic viscosity [m^2/s]

Subscripts

c	Convection
d	Droplet
ev	Evaporation
imp	Impact
int	Internal
r	Radiation
s	Steam
sat	Saturation
w	Wall

REFERENCES

1. A. V. S. Oliveira. et al., "Parametric effects on the flow redistribution in ballooned bundles evaluated by magnetic resonance velocimetry," *Experimental Thermal and Fluid Science*, **125**, pp. 110383 (2021)

2. A. V. S. Oliveira et al., "Velocity field and flow redistribution in a ballooned 7×7 fuel bundle measured by magnetic resonance velocimetry," *Nucl. Eng. Des.*, **369**, pp. 110828 (2020)

3. A. V. S. Oliveira, J. D. Peña Carrillo, A. Labergue, T. Glantz, and M. Gradeck, "Mechanistic modeling of the thermal-hydraulics in polydispersed flow film boiling in LOCA conditions," *Nucl. Eng. Des.*, **357**, pp. 110388 (2020)

4. P. Ruyer et al., "Two-phase flow across a partially damaged core during the reflood phase of a loca," *Nuclear Engineering and Design*, **264**, pp. 187–194 (2013)

5. J. D. Peña Carrillo, A. V. S. Oliveira, A. Labergue, T. Glantz, and M. Gradeck, "Experimental thermal hydraulics study of the blockage ratio effect during the cooling of a vertical tube with an internal steam-droplets flow," *Int. J. Heat Mass Transf.*, **140**, pp. 648 – 659 (2019)

6. Y. Jin, F.-B. Cheung, S. M. Bajorek, K. Tien, and C. L. Hoxie, "Investigation of the thermal-hydraulic non-equilibrium in a 7x7 rod bundle during reflood," *International Journal of Heat and Mass Transfer*, **127**, pp. 266 – 279 (2018)

7. Y. Jin et al., "Experimental study of droplet sizes across a spacer grid location under various reflood conditions," *Experimental Thermal and Fluid Science*, **94** (February 2017), pp. 246–257 (2018)

8. Y. Jin et al., "Development of a droplet breakup model for dry spacer grid in the dispersed flow film boiling regime during reflood transients," *International Journal of Heat and Mass Transfer*, **143**, pp. 118544 (2019)

9. T. Glantz et al., "DRACCAR: A multi-physics code for computational analysis of multi-rod ballooning, coolability and fuel relocation during LOCA transients Part one: General modeling description," *Nuclear Engineering and Design*, **339** (June), pp. 269–285 (2018)

10. G. Repetto, T. Glantz, G. Guillard, B. Bruyère, and Q. Grando, "Core coolability in Loss Of Coolant Accident: the COAL experiments investigating the thermal hydraulics of a rod bundle with blocked area during the reflooding," *17th International Topical Meeting on Nuclear Reactor Thermal Hydraulics (NURETH-17)*, **1**, pp. 359–372 (2017)

11. G. Repetto, C. Marquié, B. Bruyère, and T. Glantz, "Core coolability in loss of coolant accident: the COAL experiments," *16th International Topical Meeting on Nuclear Reactor Thermal Hydraulics (NURETH-16)*, **1**, pp. 24–37 (2015)

12. V. Gnielinski, "New equations for heat and mass transfer in the turbulent flow in pipes and channels," *Int. J. Chem. Eng.*, **16** (2), pp. 359 – 368 (1976)

13. W. R. Ranz, W. E. and Marshall, "Evaporation from drops," 1952

14. M. C. Yuen and L. W. Chen, "Heat-transfer measurements of evaporating liquid droplets," *Int. J. Heat Mass Transf.*, **21** (5), pp. 537–542 (1978)

15. M. Gradeck, N. Seiler, P. Ruyer, and D. Maillet, "Heat transfer for Leidenfrost drops bouncing onto a hot surface," *Exp. Therm. Fluid Sci.*, **47**, pp. 14 – 25 (2013)

16. A.-L. Biance, F. Chevy, C. Clanet, G. Lagubeau, and D. Quéré, "On the elasticity of an inertial liquid shock," *Journal of Fluid Mechanics*, **554**, pp. 47–66 (2006)

17. G. Hewitt and A. Govan, "Phenomenological modelling of non-equilibrium flows with phase change," *Int. J. Heat Mass Transf.*, **33** (2), pp. 229 – 242 (1990)

18. Y. Guo and K. Mishima, "A non-equilibrium mechanistic heat transfer model for post-dryout dispersed flow regime," *Ep. Therm. Fluid Sci.*, **26** (6-7), pp. 861–869 (2002)

19. K. H. Sun, J. M. Gonzales-Santalo, and C. L. Tien, "Calculation of Combined Radiation and Convection Heat Transfer in Rod Bundles Under Emergency Cooling Conditions," *Int. J. Heat Mass Transf.*, **98** (3), pp. 414–420 (1976)

20. W.-H. Chou and G. Faeth, "Temporal properties of secondary drop breakup in the bag breakup regime," *Int. J. Multiph. Flow*, **24** (6), pp. 889 – 912 (1998)

21. A. V. S. Oliveira, J. E. Luna Valencia, T. Glantz, G. Repetto, and M. Gradeck, "Etude du refroidissement d'une zone représentative d'un assemblage de cœur de REP / Study of the cooling of a PWR's core assembly representative zone .," *Proc. Congrès Annuel de la Société Française de Thermique 2020*, (2020)